Available online at www.sciencedirect.com
ScienceDirect
Tetrahedron
Tetrahedron 63 (2007) 3471–3482

1,N^6-Etheno-2′-deoxytubercidin and pyrrolo-C: synthesis, base pairing, and fluorescence properties of 7-deazapurine nucleosides and oligonucleotides

Frank Seela,[a,b,*] Enno Schweinberger,[a] Kuiying Xu,[a,b] Venkata Ramana Sirivolu,[a,b] Helmut Rosemeyer[a] and Eva-Maria Becker[a]

[a]*Laboratorium für Organische und Bioorganische Chemie, Institut für Chemie, Universität Osnabrück, Barbarastr. 7, 49069 Osnabrück, Germany*
[b]*Laboratory of Bioorganic Chemistry and Chemical Biology, Center for Nanotechnology, Heisenbergstraße 11, 48149 Münster, Germany*

Received 28 June 2006; revised 21 September 2006; accepted 21 September 2006
Available online 2 February 2007

Abstract—The synthesis of 1,N^6-etheno-7-deaza-2′-deoxyadenosine (**12b**) which was prepared from 7-deaza-2′-deoxyadenosine (**5a**) with chloroacetaldehyde is described. Also the regioselective glycosylation of the 7-deazapurine-2-one at nitrogen-1 (**19**) furnishing the pyrrolo-C nucleoside **7a** is reported and a side chain derivative with a terminal triple bond (**7d**) is prepared. The fluorescence properties of these nucleosides and related compounds were determined. The etheno nucleoside **12b** is strongly fluorescent showing a Stokes shift of 134 nm and a quantum yield of Φ=0.53. It proved to be stable, both in acidic and in alkaline medium while the parent purine compound **10b** is labile under both conditions. Compound **12b** was converted into its phosphoramidite **14** and was incorporated into oligonucleotides. Compound **12b** destabilizes oligonucleotide duplexes when it is located in the center of the molecule; it stabilizes when it is incorporated in the terminal base pair or acts as an overhanging nucleoside. Temperature-dependent fluorescent measurements yielded sigmoidal melting profiles when compound **12b** is stacked to the terminal base pair while a linear decrease of the fluorescence is observed when the molecule is located opposite to the four canonical nucleosides in the center of the duplex.

1. Introduction

Canonical bases of nucleic acids are virtually non-fluorescent at rt showing only significant emission in frozen glasses or at extreme pH values.[1] By contrast modified derivatives such as purin-2-amine, purin-2,6-diamine, 2-oxopurine, and their nucleosides (**1a–c**)[2] as well as pyrrolo[2,3-*d*]-pyrimidine analogues (**2a–c**)[3–5] are fluorescent in neutral aqueous solution (purine numbering is used throughout Section 2). Guanosine and its 2′-deoxy derivative become fluorescent when the base is methylated at the 7-position (**3a**,**b**),[6a] or when a nitrogen is introduced in the 8-position,[6b] while the non-charged 7-deazapurine derivative **4** is not fluorescent[7,8] (Scheme 1). The corresponding 7-deaza-2′-deoxyadenosine (**5a**) develops fluorescence, when alkenyl- or alkynyl side chains are introduced at the 7-position (**5b**,**c**)[9] or when the aromatic system is enlarged as in compound **6**.[10,11]

Other fluorescent 7-deazapurine derivatives are the pyrrolo-C nucleosides such as **7b**[12] containing the same heterocycle as the fluorescent nucleoside **2c**[5] but with nitrogen-1 as the glycosylation position. While pyrrolo-C can be considered as a pyrimidine–pyrrol ring annelation product with a [2,3-*d*] ring connectivity, the related etheno-C nucleosides **8a**,**b**[13–15] show a ring annelation via the [1,2-*c*] sites. A naturally occurring fluorescent nucleoside containing structural elements of the ethenonucleosides is wyosine (**9a**).[16,17] As it is hydrolytically labile, a stable deaza analogue **9b** has been prepared.[18] 1,N^6-ethenoadenosine **10a** and the corresponding 2′-deoxyribonucleoside **10b**[13,19] show strong fluorescence, which is significantly decreased when an additional nitrogen is introduced in the 2-position as in compounds **11a**,**b**.[20,21] Because of their propensity to fluorescence, the ethenonucleosides **8a**,**b** and **10a**,**b** are of great value for probing the biochemical and biophysical properties of nucleosides, nucleotides, and nucleic acids. The low stability of εdA (**10b**) has prompted us to combine the favorable stability of the 7-deazapurine system with the fluorescence properties of the etheno moiety. 1,N^6-Etheno-7-deazaadenosine (1,N^6-ethenotubercidin, **12a**)[22a] has been already described. This manuscript reports on 1,N^6-etheno-7-deaza-2′-deoxyadenosine, (εc^7A_d, **12b**),[22b] its synthesis, conversion into the

Keywords: Etheno nucleosides; Pyrrolo-C nucleosides; 7-Deazapurines; Fluorescence; Base paring; Oligonucleotides.
* Corresponding author. Tel.: +49 (0)541 9692791; fax: +49 (0)541 9692370; e-mail: frank.seela@uni-osnabrueck.de
URL: http://www.seela.net

0040–4020/$ - see front matter © 2007 Elsevier Ltd. All rights reserved.
doi:10.1016/j.tet.2006.09.114

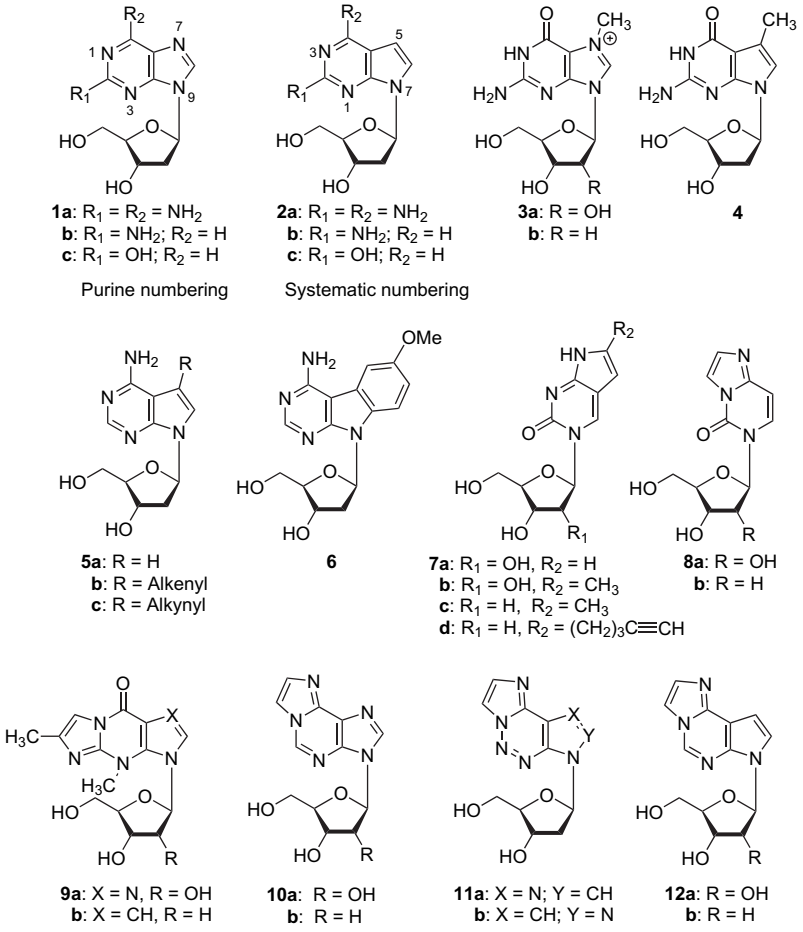

Scheme 1.

phosphoramidite **14** and its incorporation into oligonucleotides. The syntheses and fluorescent properties of pyrrolo-C ribonucleoside **7a** and the 2′-deoxyribofuranosyl derivative **7d** are also described. Hybridization studies are performed evaluating the base pairing of compound **12b** as well as the fluorescence properties of the nucleosides and oligonucleotides. For other fluorescent nucleosides including pterins we refer to reviews.[23,24]

2. Results and discussion

2.1. Synthesis and spectroscopic properties of nucleosides

Kochetkov and co-workers were the first to describe the reactions of 9-alkyladenine or 1-alkylcytosine with chloroacetaldehyde to give the N^9-alkyl 1,N^6-ethenoadenine or N^1-alkyl 1,N^4-ethenocytosine.[25] Later, Leonard and coworkers performed this reaction on adenosine (→**10a**) and AMP.[13,26] Afterwards 1,N^6-etheno-2′-deoxyadenosine (**10b**) has been prepared.[14] In 1980 the Townsend group reported the synthesis of certain fluorescent imidazo[1,2-*c*]pyrrolo-[3,2-*e*]pyrimidine ribonucleosides (≡1,N^6-etheno-7-deazaadenosine, **12a**).[20,24] The reaction of 7-deaza-2′-deoxyadenosine (**5a**)[27] with chloroacetaldehyde (18 h, 30 °C) is now undertaken furnishing 1,N^6-etheno-2′-deoxytubercidin (**12b**, εc^7A_d) (Scheme 2). Nucleoside **12b** is extraordinarily stable to both acid and base, which is in contrast to the labile purine congener **10b**. Compound **10b** has a half-life of 21 min in 25% aqueous ammonia at 40 °C and of less than 1 min in 6 N aqueous HCl at rt, while compound **12b** has half-lives of 85 and 9.8 h under corresponding conditions. The acid stability results from the hydrolytically stable N-glycosylic bond of 7-deazapurine nucleosides, while the stability in alkaline medium is due to a slow ring opening at position 2 of the modified base. This makes compound **12b** superior to its 'purine' counterpart **10b** and asks for its application as fluorescent probe in oligonucleotide chemistry and biology. Thus, the introduction of a 4,4′-dimethoxytrityl group into **12b** was performed under standard conditions[28] resulting in the DMT derivative **13** (73% yield). Phosphitylation[29]of **13** with chloro-(2-cyanoethoxy)-*N*,*N*-diisopropylaminophosphine afforded the phosphoramidite **14** (Scheme 2).

Next, two other fluorescent 7-deazapurine nucleosides were prepared, namely the pyrrolo-C/dC compounds **7a** and **7d**. Usually, the synthesis of pyrrolo-C nucleosides uses an iodinated pyrimidine nucleoside and an alkyne as precursors employing the *Sonogashira* cross coupling reaction followed by cyclization and ammonolysis of the furano intermediate.[30,31] We performed the same reaction with the 5-iodo nucleoside **15** (Scheme 3) and 1,6-heptadiyne, as such compound allows further functionalization at the terminal triple bond. An excess amount of diyne is employed to

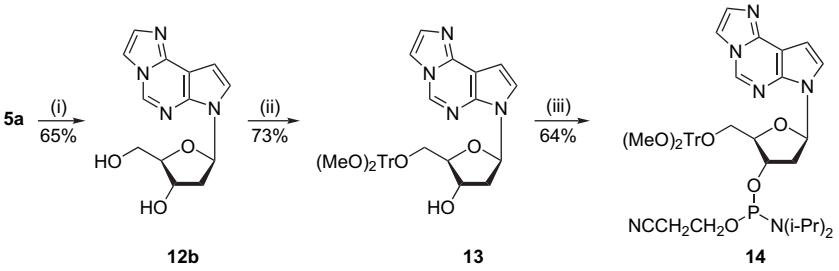

Scheme 2. Reagents and conditions: (i) $ClCH_2CHO$, 18 h, 30 °C; (ii) $(MeO)_2TrCl$, pyridine, 4 h, rt; (iii) *i*-$Pr_2NP(Cl)OCH_2CH_2CN$, *i*-Pr_2EtN, CH_2Cl_2, rt.

avoid the bis-functionization.[32] Already during this reaction the formation of a minor amount of the cyclized furanopyrimidine **17** was observed. This derivative was already reported in the literature but was formed in only 4% yield.[33] Hence, the intermediate **16** was isolated and then cyclized by treatment with CuI, affording compound **17** in 90% yield. It was then transformed to the corresponding pyrrolo[2,3-*d*]pyrimidine nucleoside **7d** (25% aq ammonia). The advantage of this reaction route is the use of the readily available 5-iodouridine or its 2′-deoxy derivative as starting materials. A drawback of the procedure is the use of the palladium catalyst employed in the cross coupling reaction. This makes the process not only costly, but also troublesome for the difficulty to remove traces of metals from the final nucleoside. Therefore, we have developed an alternative route. Direct glycosylation of the silylated (*N*,*O*-bis(trimethylsilyl)acetamide, BSA) pyrrolo[2,3-*d*]pyrimidin-2(3*H*)-one (**19**) with the acylated sugar derivative **20** in acetonitrile in the presence of trimethylsilyl triflate as catalyst (one-pot Vorbrüggen reaction) afforded the protected nucleoside **21** in 87% yield (Scheme 4). The regioselective glycosylation at the lactam moiety without involving the nitrogen of the five-membered ring is the result of the low nucleophilicity of the pyrrol nitrogen. The position of glycosylation was confirmed by ^{13}C NMR spectra, which are almost identical to the methyl derivative **7c**,[31] except that carbon-8 is shifted downfield by about 10 ppm, which is typical for the methyl substitution. Deblocking of **21** with NaOMe–MeOH resulted in the pyrrolo-nucleoside **7a** (81% yield). This compound was identical to a compound **7a**, which was obtained from 5-ethynyluridine by the same reaction route as described for **7d**, which is verified by the HPLC and UV profiles. All compounds were characterized by ^1H and ^{13}C NMR spectra as well as by elemental analysis. ^{13}C NMR signals were assigned by gated-decoupled ^{13}C NMR spectra (Table 1) as well as in some cases by DEPT-135 and CH HETCOR spectra.

Next, the photophysical properties of all new compounds as well as of related nucleosides were examined. This includes

Table 1. ^{13}C NMR chemical shifts (δ) of nucleosides measured in DMSO-d_6 at 298 K

Compd	C(2)[a] / C(2)[b]	C(4)[a] / C(7a)[b]	C(5)[a] / C(4a)[b]	C(6)[a] / C(4)[b]	C(7)[a] / C(5)[b]	C(8)[a] / C(6)[b]	C(10)[a]	C(11)[a]	C(1′)	C(2′)	C(3′)	C(4′)	C(5′)
							C≡C[c]						
2c	155.7	158.1	108.1	140.0	101.4	126.6			81.9	—[d]	70.9	87.1	61.9
7a	154.1	158.7	107.4	137.3	100.5	127.4			91.1	74.9	68.4	84.1	59.8
7c	153.7	159.2	108.9	134.0	96.8	137.7			86.5	41.2	69.9	87.6	61.0
7d	153.7	159.1	108.6	134.5	96.5	141.1	83.7	71.6	86.6	41.3	69.6	87.6	61.9
12b	135.0	138.8	106.1	141.6	99.9	122.5	132.1	111.2	83.3	—[d]	70.9	87.3	61.9
13	135.0	138.8	106.3	141.5	99.9	122.5	132.1	111.2	83.3	—[d]	70.7	85.4	61.4
16	149.4			161.7	98.8	142.8	92.2	83.7	84.5	—[d]	70.1	87.5	60.9
							73.4	71.7					
17	157.9	171.8	106.9	137.6	101.0	154.5	84.3	72.5	88.0	41.8	70.3	88.7	61.4
19	156.1	159.5	107.7	139.3	100.3	126.5							
21	153.6	159.5	108.7	138.7	100.5	128.2			92.5	74.4	70.7	79.2	63.7

[a] Purine numbering.
[b] Systematic numbering.
[c] Triple bond carbons for compounds **7d**, **16**, and **17**.
[d] Superimposed by the signal of DMSO-d_6.

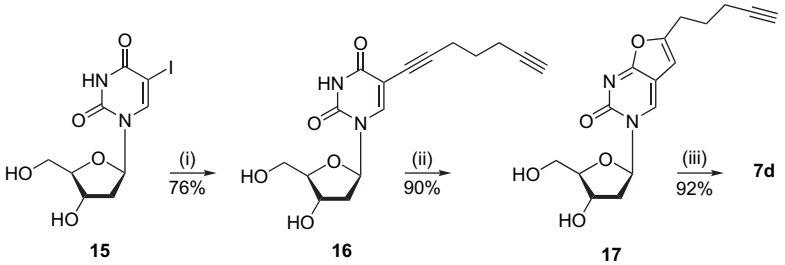

Scheme 3. Reagents and conditions: (i) 1,6-heptadiyne, $[Pd(PPh_3)_4]$, CuI, Et_3N–DMF, rt; (ii) Et_3N–MeOH, 80 °C; (iii) 25% aq NH_3, rt, overnight.

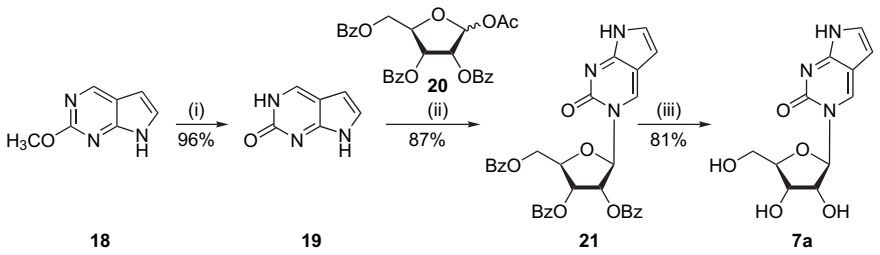

Scheme 4. Reagents and conditions: (i) HCl–H_2O; (ii) BSA, TMSOTf, 80 °C; (iii) NaOMe, rt.

the determination of the fluorescence data and quantum yields. Under neutral conditions, compound **12b** shows two UV maxima at 289 nm (ε 6000) and 275 nm (ε 5700), compared to 294 nm (ε 3100), 275 nm (ε 6000), 265 nm (6000), and 258 (5000) nm for **10a** (water, pH 7).[13] The pK_a value of protonation is 5.3 for 1,N^6-etheno-2′-deoxy-7-deazaadenosine (**12b**) and 3.9 for 1,N^6-etheno-2′-deoxyadenosine (**10b**).[34] Figure 1(a) shows the excitation and emission spectrum of εdA (**10a**) while the spectra of εc^7A_d (**12b**) are displayed in Figure 1(b). The *Stokes* shift of compound **12b** is by 25 nm larger than that of **10a**, while the emission maximum of the 7-deazapurine **12b** is shifted bathochromically by 9 nm (Table 2). Between pH 6 and 14 the fluorescence intensity of **12b** is constant while it is quenched by protonation under stronger acidic conditions (data not shown). The favorable photophysical characteristics and the higher chemical stability of 7-deazapurine nucleosides make compound **12b** superior to the purine compound **10b**, in particular when the compound has to be used in solid-phase oligonucleotide synthesis employing the protocol of phosphoramidite chemistry.

Also, quantum yields were measured for the nucleosides. Compounds **10a** and **12b** have almost identical quantum yields. The quantum yields of the etheno 2-azanucleosides **11a** and **11b** are significantly lower. Although it was reported for pyrrolo-C nucleosides that they are highly fluorescent, conflicting data exist on their relative quantum yield. The quantum yields reported in this manuscript refer to quinine sulfate as standard measured in 0.1 N sulfuric acid with a quantum yield of 0.53.[35] Measurements for nucleosides are performed under neutral conditions in water. Using these conditions, a quantum yield of only Φ=0.06 was obtained for compound **7a**, which is significantly lower than that of the highly fluorescent ethenonucleosides **10a** and **12b** (Φ=0.52 for **10a** and 0.53 for **12b**). The introduction of a side chain does not change the quantum yield significantly but shifts the excitation as well as the emission maximum to longer wavelength (Table 2). The corresponding furano compound **17** shows a quantum yield of Φ=0.06. It should be noted that the fluorescence of pyrrolo-C nucleosides is caused by the pyrrolo[2,3-*d*]pyrimidine functionalized with a hydroxyl group at the 2-position. We have compared

Table 2. Photophysical data of base modified nucleosides[a]

Compd	Ex. [nm]	Em. [nm]	Q.Y. [Φ]
1b	304	365	0.84
1c	313	376	0.24
2b	311	393	0.47
2c	329	436	0.15
7a	336	450	0.06
7d	340	456	0.04
10a	300	409	0.52
11a	349	481	0.05
11b	300	441	0.14
12b	284	418	0.53
17	322	410	0.06
19	329	436	0.12

[a] Measured in H_2O; quinine sulfate in 0.1 N H_2SO_4 as standard with Φ=0.53.[35]

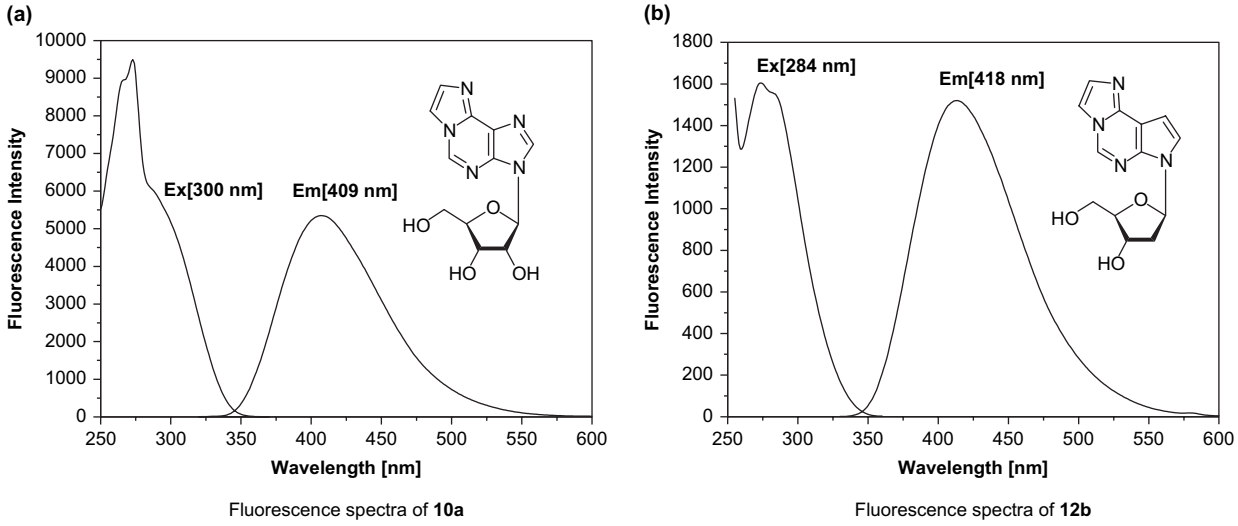

Figure 1. Steady-state excitation and emission spectra of nucleosides **10a** (a) and **12b** (b) measured in water at room temperature.

the fluorescence data of **2c** with those of **7a**, **7d**, and **19**. According to this, the quantum yield of the base **19** as well as of the N^9-glycosylated compound **2c** is higher than that of the pyrrolo-C **7a** (Table 2). It can also be concluded that a 2-amino group causes higher quantum yields than a 2-hydroxy group (**1b**, **2b** vs **1c**, **2c**).

2.2. Synthesis and properties of oligonucleotides containing 1,N^6-etheno-7-deaza-2′-deoxyadenosine (12b)

Oligonucleotides containing compound **12b** were synthesized employing the phosphoramidite **14** (for details of synthesis and characterization, see Section 4). To investigate the base pairing and the fluorescence properties, the complementary oligonucleotides 5′-d(TAG GTC AAT ACT) (**22**) and 3′-d(ATC CAG TTA TGA) (**23**) were used as reference.[36] A single incorporation of the etheno nucleoside **12b** into the duplex 5′-d(TAGGTC**12b**ATACT) (**24**)·3′-d(ATCCAG**X**TATGA) (**X**=dA, dG, dT, dC; **23**, **25**–**27**) located in the center of the molecule reduces the T_m value by 9 or 10 °C depending on the four canonical nucleosides located opposite to the modified nucleoside. The incorporation of two consecutive εc^7A_d (**12b**) residues (**30**·**23**) shows a reduction of the T_m value to the parent duplex by 21 and 22 °C, respectively, in low or high salt buffer solution (Table 3). As expected, the T_m-decrease is less pronounced when the two **12b** residues are separated (**29**) compared to the consecutive incorporations (**30**) (Table 3). The behavior of the T_m values implies the absence of a base pair. The T_m values of oligonucleotide duplexes containing the etheno 7-deaza-purine derivative **12b** are similar to those of the parent purine derivative **10b** (Table 3).

Recently a base pair of guanine and 1,N^6-ethenoadenine was detected in an oligonucleotide duplex by X-ray crystallography.[37] According to the almost identical T_m values found for oligonucleotide duplexes containing **10b** or **12b** (Table 3), a tridentate base pair which was reported for the crystal (Scheme 5(a)) is unlikely to be formed in solution. Only a bidentate base pair as shown in Scheme 5(b) can be considered as the oligonucleotide duplexes containing **10b** or **12b** show the same stability. As the T_m values of the ethenonucleosides are decreasing by 7–11 °C compared to reference duplex **22**·**23** with dA–dT at that position, the decrease is in the range of a substitution by an abasic residue. Therefore, there is very little evidence for a base pair formed in solution. It is much more likely that the stabilizing effect of compound **12b** results from stacking forces. The universal character of the pairing with all four DNA constituents supports this assumption.

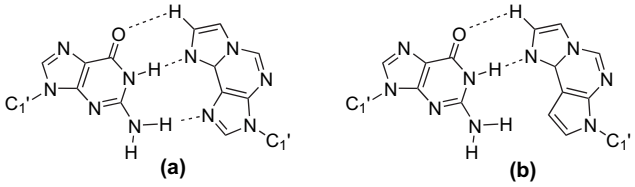

Scheme 5. Base pair motifs suggested for **10b** with dG[37] and for the related **12b**.

The blunt-end duplex containing a single εc^7A_d-dT base pair at the terminus (**28**·**22**) was prepared (Table 3). Its T_m value is found to be 49 or 54 °C (depending on the buffer system) and is therewith 2–4 °C higher than that of the parent duplex **22**·**23**. Apparently, the increased surface area of **12b** causes strong stacking interaction of the tricyclic base with the last intact base pair. As these stacking forces are stronger than the hydrogen bonding of a dA–dT base pair, the T_m value of **22**·**28** is higher than that of **22**·**23** with the consequence that the terminal dT forms a dangling end without any interaction. Part of the strong stacking of **12b** is due to its hydrophobic character, which was verified by a significantly reduced mobility on *RP-18* HPLC compared to that of the nucleoside **5a** (Fig. 2).

In order to quantify the stabilizing effect of **12b** as a dangling end, a series of oligonucleotide duplexes were synthesized in which the etheno nucleoside **12b** was added as an unpaired nucleotide either to the 5′ site or the 3′-end of a single stranded oligonucleotide, which was then hybridized with its complement (**35**–**37**, Table 4). This allows the determination of the stacking forces independent of hydrogen bonding (Fig. 8D). T_m measurements of the resulting duplexes (Table 4) revealed some interesting features. One overhanging

Table 3. T_m values and thermodynamic data of oligonucleotide duplexes containing **12b**, **10b**, **5a** and of the corresponding reference duplexes

Duplex		T_m [°C]	ΔG_{310} [kcal/mol]	Duplex		T_m [°C]	ΔG_{310} [kcal/mol]
5′-d(TAGGTCAATACT)	**22**	47[a]	−10.4[a]	5′-d(TAGGTC**10b**ATACT)	**31**	34[a]	−7.0[a]
3′-d(ATCCAGTTATGA)	**23**	50[b]	−11.1[b]	3′-d(ATCCCG C TATGA)	**25**		
5′-d(TAGGTC**12b**ATACT)	**24**	36[a]	−7.3[a]	5′-d(TAGGTC**10b**ATACT)	**31**	40[a]	−8.5[a]
3′-d(ATCCAG C TATGA)	**25**	38[b]	−7.9[b]	3′-d(ATCCCG G TATGA)	**26**		
5′-d(TAGGTC**12b**ATACT)	**24**	40[a]	−8.2[a]	5′-d(TAGGTC**10b**ATACT)	**31**	38[a]	−7.9[a]
3′-d(ATCCAG G TATGA)	**26**	40[b]	−8.5[b]	3′-d(ATCCCG A TATGA))	**27**		
5′-d(TAGGTC**12b**ATACT)	**24**	39[a]	−7.7[a]	5′-d(TAGGTC**10b**ATACT)	**31**	35[a]	−7.5[a]
3′-d(ATCCAG A TATGA)	**27**	40[b]	−8.8[b]	3′-d(ATCCCG T TATGA)	**23**		
5′-d(TAGGTC**12b**ATACT)	**24**	38[a]	−7.7[a]	5′-d(T**5a**GGTC**5a**ATACT)	**32**	41[a]	−8.9[a]
3′-d(ATCCAG T TATGA)	**23**	40[b]	−8.4[b]	3′-d(ATCC**5a**GTT**5a**TGA)	**33**		
5′-d(TAGGTCAATAC T)	**22**	49[a]	−11.0[a]				
3′-d(ATCCAGTTATG**12b**)	**28**	54[b]	−12.1[b]				
5′-d(T**12b**GGTCAAT**12b**CT)	**29**	37[a]	−7.9[a]				
3′-d(A T CCAGTTA T GA)	**23**	43[b]	−8.8[b]				
5′-d(TAGGTC**12b12b**TACT)	**30**	25[a]	−5.7[a]				
3′-d(ATCCAG T T ATGA)	**23**	29[b]	−6.3[b]				

[a] Determined in 10 mM Na cacodylate, 10 mM $MgCl_2$, 100 mM NaCl, pH 7.
[b] Determined in 60 mM Na cacodylate, 100 mM $MgCl_2$, 1 M NaCl, pH 7.

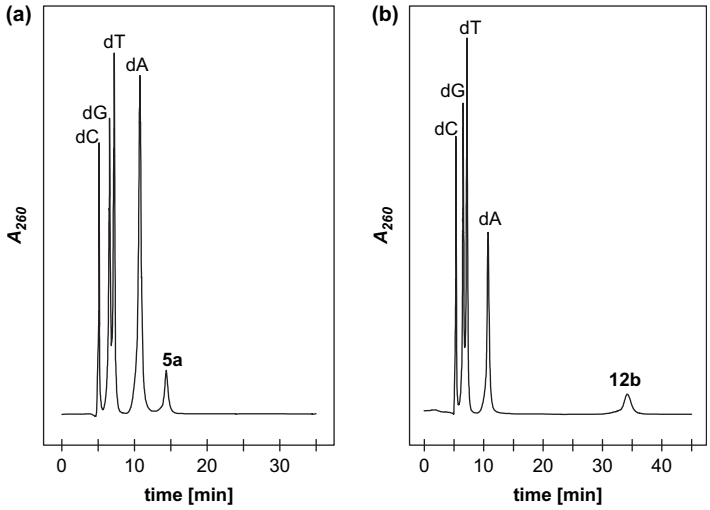

Figure 2. (a) HPLC profile of the nucleosides of the oligomer **32** after enzymatic hydrolysis. The nucleoside mixture was analyzed by *RP-18* HPLC at 260 nm on an *RP-18* column (250-4, 5 μm). Gradient: 0.1 M (Et_3NH)OAc (pH 7.0)–MeCN 90:10, flow rate 1.0 mL/min. (b) HPLC profile of nucleosides of the oligomer **29** after enzymatic hydrolysis. For details see (a).

εc^7A_d (**12b**) residue enhances the T_m value of the parent duplex **22**·**23** by 3–5 °C (depending on the buffer system). The same enhancement is found for the corresponding DNA–RNA hybrid **22**·**34**. Introduction of two pending εc^7A_d (**12b**) residues, one on each end of the strand (**36**·**35**) doubles the T_m increase to 7–8 °C. Pending of a compound **12b** tail on one end of the double helix (**22**·**37**) gives the same stabilization as a single **12b** residue at the same position. In order to compare the stacking force of compound **12b** with that of other modified nucleobases it was linked to the self-complementary oligomer 5′-d(CGCGCG) (**40**) giving **41**.[38] The duplex **41**·**41** exhibits a 12 °C higher T_m value than the parent **40**·**40** (Table 4).

Recently, we have reported on a linear correlation of the ΔT_m of normal duplexes and those with dangling nucleosides as function of the molecular polarizability α_m.[39] The corresponding values for **12b** fit to this correlation. The stacking force of **12b** ranges between that of phenanthrene and pyrene, which have been attached to **40**·**40** before by others.[40] The remarkable stabilizing effect of **12b** as dangling nucleoside prompted us to study this property also on oligomers with other structures. The oligomer 5′-d(GCGAAGC) (**42**) forms an extraordinarily stable minihairpin with a T_m value of 38 °C in a 1:1 mixture (v/v) of formamide/(10 mM Na cacodylate, 100 mM NaCl, 10 mM $MgCl_2$, pH 7).[41] Addition of a single **12b** residue to the 5′-terminus enhances

Table 4. T_m values and thermodynamic data of oligonucleotide duplexes with **12b** as dangling residue and of reference oligomers

Duplex		T_m [°C]	ΔG_{310}[a]	Duplex		T_m [°C]	ΔG_{310}[a]
5′-d(TAGGTCAATACT)	**22**	47[b]	−10.4[b]	5′-d(aL-**12b**TAGGTCAATACT)[d]	**39**	48[b]	−11.2[b]
3′-d(ATCCAGTTATGA)	**23**	50[c]	−11.1[c]	3′-r(AUCCAGUUAUGA)	**34**		
5′-d(TAGGTCAATACT)	**22**	45[b]	−10.2[b]	5′-d(aL-**12b**TAGGTCAATACT)[d]	**39**	53[b]	−13.2[b]
3′-r(AUCCAGUUAUGA)	**34**	48[c]	−10.4[c]	3′-r(AUCCAGUUAUGA**12b**)	**35**		
5′-d(TAGGTCAATACT)	**22**	51[b]	−12.0[b]	5′-d(CGCGCG)	**40**	47[b]	−8.4[b]
3′-d(ATCCAGTTATGA**12b**)	**35**	55[c]	12.8[c]	3′-d(GCGCGC)	**40**	46[c]	−8.2[c]
5′-d(**12a**TAGGTCAATACT)	**36**	50[b]	−11.7[b]	5′-d(**12b**CGCGCG)	**41**	59[b]	−10.9[b]
3′-d(ATCCAGATATGA)	**23**	55[c]	−12.5[c]	3′-d(GCGCGC**12b**)	**41**	61[c]	−11.0[c]
5′-d(**12b**TAGGTCAATACT)	**36**	54[b]	−13.1[b]	A G C G-5′ A G C-3′	**42**	38[e]	−0.04[e]
3′-d(ATCCAGTTATGA**12b**)	**35**	58[c]	−13.9[c]				
5′-d(TAGGTCAATACT) 3′-d(ATCCAGTTATGA(**12b**)$_3$)	**22** **37**	50[b]	−12.3[b]	A G C G **12b**-5′ A G C-3′	**43**	49[e]	−0.9[e]
5′-d(**12b**TAGGTCAATACT)	**36**	48[b]	−10.7[b]	5′-d(AGT ATT GAG GAT)	**44**	42[b]	−9.1[b]
3′-r(ATCCAGUUAUGA)	**34**			5′-d(TNA TAA NTN NTA)[f]	**45**		
5′-d(aL-TAGGTCAATACT)[d]	**38**	46[b]	−10.7[b]	5′-d(**12b**AGT ATT GAG GAT)	**46**	46[b]	−10.9[b]
3′-d(AUCCAGTTATGA)	**23**			5′-d(TNA TAA NTN NTA)[f]	**45**		
5′-d(aL-TAGGTCAATACT)[d]	**38**	46[b]	−10.5[b]	5′-d(AGT ATT GAG GAT)	**44**	43[b]	−9.2[b]
3′-r(ATCCAGATATGA)	**34**			5′-d(**12b**TNA TAA NTN NTA)[f]	**47**		
5′-d(aL-**12b**TAGGTCAATACT)[d]	**39**	49[b]	−11.4[b]				
3′-d(ATCCAGTTATGA)	**23**						

[a] In kcal/mol, 1 cal=4.184 J.
[b] Determined in 10 mM Na cacodylate, 10 mM $MgCl_2$, 100 mM NaCl, pH 7.
[c] Determined in 60 mM Na cacodylate, 100 mM $MgCl_2$, 1 M NaCl, pH 7.
[d] aL=NH_2–$(CH_2)_6$, an amino linker.
[e] Determined in 1:1 (v/v) mixture of formamide and 10 mM Na cacodylate, 100 mM NaCl, 10 mM $MgCl_2$, pH 7; oligomer concentration: 5 μM of each single strand.
[f] N=2′-deoxy-5-methylisocytidine.

the melting temperature by 11 °C (Table 4). Also, the stabilizing effect of compound **12b** on a duplex (**44**·**45**) with parallel strand orientation was measured, which exhibits a T_m value of 42 °C.[42] Attachment of a single εc^7A_d (**12b**) residue to either the 5′-end of **44** or the 5′-end of **45** leads to a slightly different stabilization of either 4 °C or 1 °C, depending on the nature of the (n-1) nucleotide. If this (n-1) nucleotide is a pyrimidine residue (dT), the T_m enhancement is low; if it is a purine base (dA), the enhancement is high. This is different from antiparallel stranded oligomers where the effect on the stability is almost identical, regardless of the (n-1) base (Table 4).

As compound **12b** might be useful for fluorescence labeling of oligonucleotides bound to polymer surfaces (biochips), we have prepared the single strand **39** containing a 5′-amino linker followed by one **12b** residue. This was hybridized with the DNA or RNA complement. For comparison also the oligomer **38** which contains only a 5′-amino linker was synthesized. T_m measurements of the duplexes (Table 4) show that the addition of the amino linker function decreases the stability only slightly (−1 °C) and that introduction of one εc^7A_d (**12b**) residue leads to a T_m increase by 3 °C. If the complementary strand is also labeled with a εc^7A_d (**12b**) moiety (**39**·**35**), the total T_m increase amounts to 7 °C. In all cases the purity of the oligonucleotides was confirmed by the detection of a single peak (>99% area) in the HPLC profile. Furthermore, MALDI-TOF spectra (Table 5) and enzymatic analysis (data not shown) confirmed the composition.

2.3. Fluorescence properties of oligonucleotides containing 1,N^6-etheno-7-deaza-2′-deoxyadenosine (12b)

In a first series of experiments, the temperature dependence of the fluorescence was measured on the single strand 5′-d(TAG GTC **12b**AT ACT) (**24**) with the etheno nucleoside **12b** in the center of the molecule. Figure 3 displays the temperature-dependent fluorescence emission profile measured at 419 nm. The graph shows a linear dependence, which is typical for fluorescent single stranded oligonucleotides. The excitation spectrum of **24** is given in Figure 4. As can be seen it exhibits no minimum around 260 nm like the spectrum of the monomer (Fig. 1B vs 4); this points to a base-to-base energy transfer[43] from the neighboring bases to the etheno base. This mechanism is verified by the fact that at higher temperature (59 °C) at which the energy transfer is hampered by the thermal motion the spectrum of the oligomer resembles more that of the monomer. This effect becomes particularly obvious when the values of relative fluorescence at 59 °C are multiplied with the factor 1.8 in order to compensate for the usual fluorescence decrease with the temperature (Fig. 4). As can be seen, the spectrum of **24** at 23 °C and the corrected one at 59 °C coincide over a wide range; differences were only observed in the range of λ_{Ex}=255–295 nm.

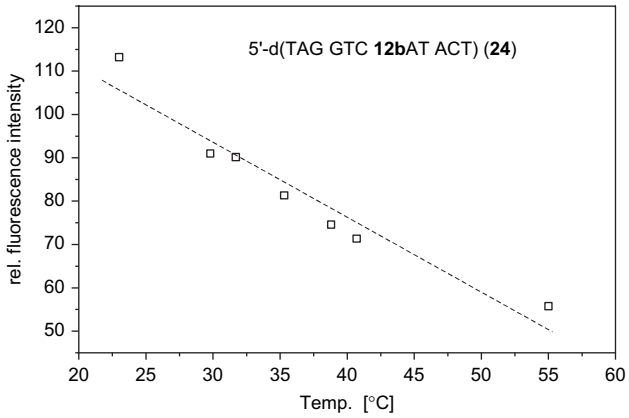

Figure 3. Dependence of the fluorescence emission of the single strand 5′-d(TAG GTC **12b** AT ACT) (**24**) on the temperature. Concentration of the oligomer: 5 μmol in 0.1 M NaCl, 0.01 M $MgCl_2$, 0.01 M Na cacodylate, pH 7.0. The emission was detected at 419 nm.

The duplex **24**·**23** exhibits a linear temperature decrease of the fluorescence emission at 419 nm; no inflection point can be observed (data not shown). The same result is observed also for the duplexes containing central **12b**-dC, **12b**-dG or **12b**-dA base pairs as well as for the oligonucleotide duplex **30**·**23** containing two consecutive **12b** residues (Table 4). The excitation spectrum of **24**·**23**, however, shows a significant bathochromic shift of the peak around 290 nm with increasing temperature (Fig. 5). When the λ_{max} values of the excitation spectra are plotted versus the temperature, a melting curve (Fig. 6) is obtained from which a T_m value of 38 °C can be taken, which is identical with the value measured by UV (Table 3).

Next, the duplex **36**·**35** carrying two overhanging **12b** nucleosides, one at each side, was studied with respect to

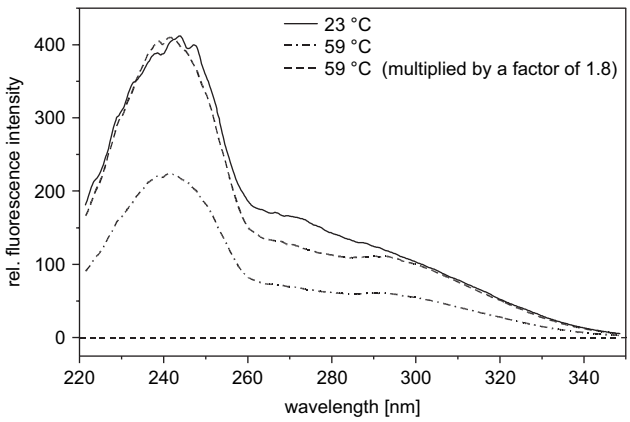

Figure 4. Temperature dependence of the excitation spectra of the single strand 5′-d(TAGGTC**12b**ATACT) (**24**). Same conditions as in Figure 3.

Table 5. Molecular masses of oligonucleotides determinated by MALDI-TOF mass spectroscopy

Oligonucleotides	$[M+H]^+$ (calcd) [Da]	$[M+H]^+$ (found) [Da]
5′-d(TAG GTC **12b**AT ACT) **24**	3668	3669
3′-d(ATC CAG TTA TG**12b**) **28**	3668	3667
5′-d(T**12b**G GTC AAT **12b**CT) **29**	3691	3692
5′-d(TAG GTC **12b12b**T ACT) **30**	3691	3689
3′-d(ATC CAG TTA TGA **12b**) **35**	3981	3981
5′-d(**12b** TAG GTC AAT ACT) **36**	3981	3982
5′-d(**12b** CGC GCG) **41**	2130	2131
5′-d(**12b**GCGAAGC) **43**	2468	2467
5′-d(**12b**AGT ATT GAG GAT) **46**	4061	4058

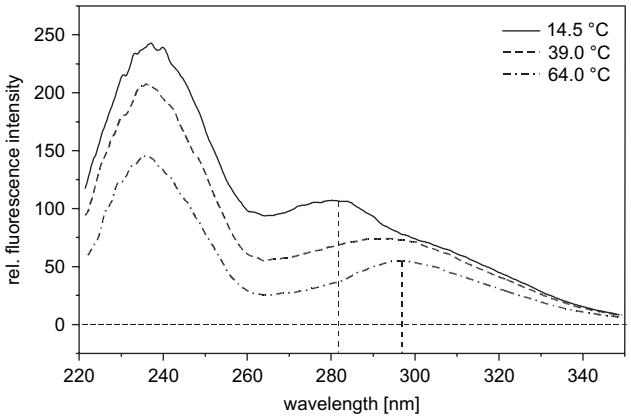

Figure 5. Excitation spectra of the duplex **24**·**23** at three different temperatures. Concentration of the oligomer **24**: 0.5 A_{260} units. Concentration of the oligomer **23**: 0.5 A_{260} units in 0.1 M NaCl, 0.01 M $MgCl_2$, 0.01 M Na cacodylate, pH 7.0.

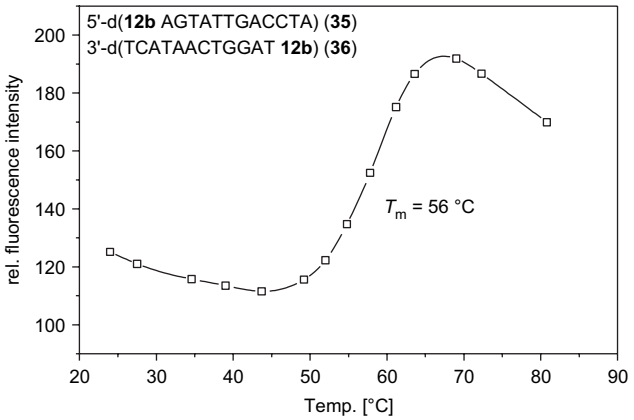

Figure 7. Temperature dependence of the fluorescence emission of the duplex **35**·**36**, with 0.5 A_{260} units of each oligomer in 1 M NaCl, 0.01 M Na_2HPO_4, pH 7.0.

temperature-dependent fluorescence emission. Here, the melting is accompanied by a strong increase of the emission and an inflection point of the curve was observed (Fig. 7) corresponding to the T_m value taken from the UV melting profile (56 °C, Table 4). Before and after the melting, the regular temperature dependence of the fluorescence emission is detected. The same phenomenon can be observed for the self-complementary duplex **41**·**41**. Also the duplex **22**·**28** which contains a terminal **12b**-dT base pair (blunt end) exhibits a fluorescence emission melting profile with a T_m value, which corresponds to that of a UV curve (data not shown).

For an undisturbed DNA mediated energy transfer between the nucleobases, a particular geometrical arrangement is of importance. Frozen as well as too flexible structures reduce the energy transfer. In the case of the duplex **24**·**23** carrying a central **12b**-dT base pair, the regular B-DNA structure is obviously distorted to such an extent that the base-to-base energy transfer is difficult (Fig. 8B). A flip out of the base as shown in Figure 8A can be ruled out as in such a situation the fluorescence emission would strongly increase during duplex formation, which is not the case. Instead, the duplex **24**·**23** exhibits fluorescence quenching. From NMR studies on duplexes containing **10b**-dT base pairs it can be seen that the bases are no longer positioned vis-à-vis but that the thymine base evades toward the neighboring base pair.[44] The base **10b** located in the interior of the helix causes in a steric clash relieved by the non-coplanar alignment across the lesion site. The neighboring pairs, therefore, might be distorted as well (Fig. 8B) in a 'domino effect' being now destabilized. The same is expected for compound **12b**. The resulting weak base interaction within the duplex might be the reason for the non-sigmoidal fluorescence change of this duplex as no significant change of the stacking of **12b** occurs during melting. However, duplexes with overhanging εc^7A_d (**12b**) residues such as **36**·**35** do not show this distortion. The overhanging base stacks to one site to the last intact base pair while overlapping both bases, the other site is surrounded by water molecules. When the duplex melts, stacking to the last intact base pair is disrupted leading to the cooperative melting indicated by the fluorescence emission curve (Fig. 7). The same phenomenon is observed for the blunt-end duplex **22**·**28** with a terminal εc^7A_d-dT base pair (Fig. 8C). In this case the thymine base is flipped out while the εc^7A_d nucleoside stacks strongly to the undecamer allowing stacking of compound **12b** with the n-1 base pair (Fig. 8C).

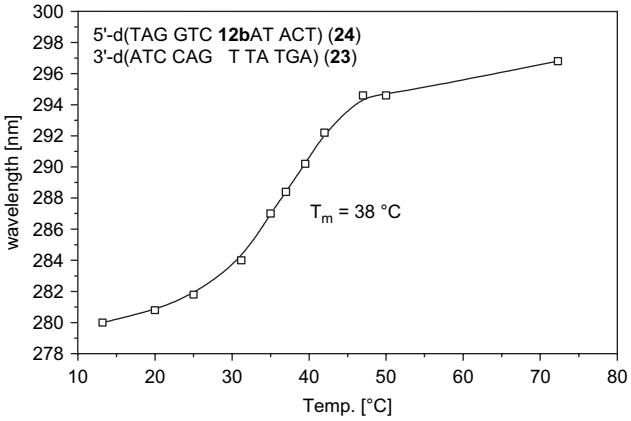

Figure 6. Temperature dependence of λ_{max} of the excitation spectrum of the duplex **24**·**23**. Same conditions as in Figure 5.

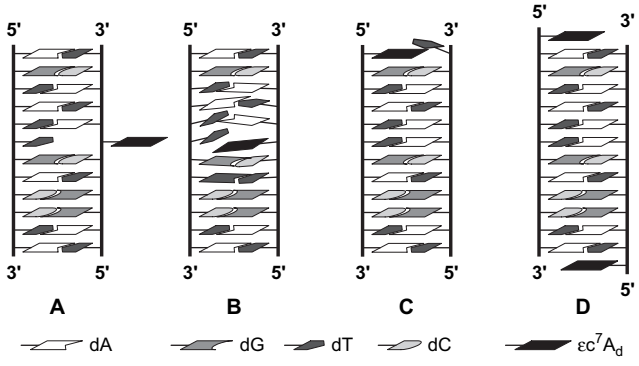

Figure 8. Possible structures of the duplexes 5′-d(TAGGTC**εc^{7}A**ATACT)·3′-d(ATCCAGTTATGA) [**A** (unlikely) and **B**], 5′-d(**εc^{7}A**GTATTGACCTA)·3′-d(TCATAACTGGAT) (**C**), 5′-d(**εc^{7}A**TAGGTCAATACT)·3′-d(ATCCAGTTATGA**εc^{7}A**) (**D**).

3. Conclusions and outlook

1,N^6-Etheno-7-deaza-2′-deoxyadenosine (εc^7A_d, **12b**) enlarges the repertoire of fluorescent compounds, namely of highly fluorescent nucleosides with a quantum yield larger than 0.5. While 1,N^6-etheno-2′-deoxyadenosine (εA_d, **10b**) is very susceptible to degradation by acid or base, compound **12b** is stable under those conditions. Two fluorescent pyrrolo-C/dC nucleosides **7a** and **7d**, which are also containing a 7-deazapurine system, were prepared by direct glycosylation or via cyclization of 5-alkynylpyrimidine nucleosides. Their fluorescence quantum yields are significantly lower ($\Phi \approx 0.05$) than those of the ethenonucleosides. Compound **12b** can be easily incorporated into oligonucleotides using the standard protocol of phosphoramidite chemistry while **10b** requires ultramild deprotection condition. Nucleoside **12b** does not pair with the canonical bases and is, therefore, a universal nucleoside. As dangling residue, it stabilizes a preformed oligonucleotide duplex. Temperature-dependent fluorescence spectra of oligonucleotide duplexes with overhanging **12b** moieties show sigmoidal melting while this is not the case for duplexes with **12b** located in the center of duplex DNA. The favorable properties of **12b** over that of **10b** make it superior as fluorescence probe to explore interactions of nucleosides and oligonucleotides.

4. Experimental

4.1. General

4.1.1. Monomers. Flash chromatography (FC): on silica gel 60 H (VWR, Darmstadt, Germany). Thin-layer chromatography (TLC): Silica Gel 60 F_{254} plates (VWR, Darmstadt); visualization by UV detection at 254 nm. Steady-state fluorescence measurements were performed on a Fluorog-3 fluorescence spectrophotometer (HORIBA Jobin Yvon Inc, USA). UV spectroscopy: U-3200 spectrophotometers (Hitachi, Japan) λ_{max} in nm, ε in dm^3/mol. NMR spectra were measured on AC-250 and AMX-500 spectrometers (Bruker, Karlsruhe). Operational frequencies: ^{1}H: 250.13 MHz, 500.14 MHz; ^{13}C: 62.896 MHz, 125.700 MHz; ^{31}P NMR: 101.256 MHz. Chemical shifts (δ values) are in parts per million relative to tetramethylsilane (^{1}H and ^{13}C NMR) as internal standard and 85% orthophosphoric acid (^{31}P NMR) as external standard. Chemical shifts (δ) in parts per million are positive when downfield shifted relative to the standard. Microanalyses were performed by Mikroanalytisches Labor Beller (Göttingen, Germany). MALDI-TOF mass spectra were recorded on a Biflex-III spectrometer (Bruker, Leipzig, Germany) in the reflector mode. The average power of the nitrogen laser (337.1 nm) at 20 Hz was 3–4 mW (150–200 μJ/pulse) with a delay time of 600 ns. Chemicals were purchased from ACROS, Fluka, or Sigma–Aldrich (Sigma–Aldrich Chemie GmbH, Deisenhofen, Germany).

4.1.2. Fluorescence measurements. All measurements were done in bi-distilled water at 20 °C. Absorption spectra were measured with a Cary 100 Bio UV–vis spectrophotometer. In order to avoid inner filter effects, the sample was not allowed to exceed 0.1 at the excitation wavelength using standard quartz cuvettes with a path length of 1 cm. Fluorescence spectra were recorded in the wavelength range between 320 and 600 nm using the Fluorog-3 fluorescence spectrophotometer (HORIBA, Jobin Yvon Inc, USA). For all calculations the water background was subtracted from the sample. The fluorescence quantum yields were determined using quinine sulfate in 0.1 N H_2SO_4 (fluorescence quantum yield 0.53)[35] as a standard with the following relation:

$$\Phi_{f.sample} = \Phi_{f.standard} \times \left(F_{sample}/F_{standard}\right) \times \left(A_{standard}/A_{sample}\right)$$

where $\Phi_{f.sample}$ is the unknown fluorescence quantum yield of the fluorophore, F is the integrated fluorescence intensity, A is the absorbance in 1 cm cuvettes and always not exceed 0.2 at and above the excitation wavelength.

4.1.3. Oligonucleotides. Oligonucleotides were synthesized with a solid-phase synthesizer, model ABI 392 (Applied Biosystems, Weiterstadt) according to the standard protocol using the 'DMT-off' mode, except for the unmodified oligodeoxynucleotides, which were synthesized using the 'DMT-on' mode. Phosphoramidites with canonical bases contained standard protecting groups. When **10b** was incorporated, phosphoramidites with the following protecting groups were employed. Pac for dA, isopropyl-Pac for dG and Ac for dC .The coupling yields were always higher than 95% (trityl monitoring). Deprotection was performed with 25% aq NH_4OH at 50 °C for 10 h. Ultramild deprotection conditions were used when **10b** was a constituent of an oligonucleotide. The detritylated modified oligomers were purified by ion-exchange chromatography on a *Dionex* Nucleopac PA-100 HPLC column (4×250 mm, P/N 043010, *Dionex* GmbH, Idstein, Germany) using the following gradient: 5 min 5% 0.01 M NaOH/1.5 M LiCl (X) in 0.01 M NaOH (Y); 25 min 5–30% Y in X; 10 min 30–5% Y in X; 5 min 5% Y in X. Ion-exchange HPLC apparatus: L 4250 UV–vis detector, L 6250 Intelligent pump, and D-2500 integrator (*Merck-Hitachi*, Germany). The tritylated unmodified oligonucleotides were purified by *RP-18* HPLC using the following apparatus and procedure: 4×250 mm *RP-18* column (*Merck*, Germany); *Merck-Hitachi* HPLC apparatus consisting of a 655 A-12 liquid chromatograph with a 655 A variable wavelength UV monitor and a D-2000 Chromato-Integrator (*Merck-Hitachi*, Darmstadt, Germany); gradients: 0.1 M (Et_3NH)OAc (pH 7.0)–MeCN 95:5 (U) and MeCN (V); gradient I: 0–50 min 0–50% V in U, flow rate 1 mL/min; gradient II: 0–20 min 0–20% V in U; 20–40 min 20–40% V in U, flow rate 1 mL/min. Detritylation was performed by treating the purified oligomers with a 2.5 % dichloroacetic acid solution in dichloromethane (1 mL) for 5 min at room temperature. After neutralization with Et_3N, evaporation to dryness, followed by co-evaporation with MeOH, the oligomers were again purified by *RP-18* HPLC using the above-mentioned device. Gradient: 0–30 min 0–20%V in U, 30–35 min 20% V in U, 35–40 min 20–0% V in U, 40–45 min 0% V in U. Subsequent desalting of all oligonucleotides was performed on an *RP-18* HPLC column (4×125 mm). Solvent for adsorption: H_2O, solvent for desorption: MeOH–H_2O 3:2. General flow rate: 1 mL/min. MALDI-TOF mass spectra of the oligonucleotides (Table 5) were measured on a Biflex-III spectrometer (Bruker, Leipzig, Germany) in the reflector mode.

The melting curves were measured on a *Cary* 1E UV–vis spectrophotometer (*Varian*, Melbourne, Australia) with a *Cary* thermoelectrical controller. The thermodynamic data (ΔH^0, ΔS^0, ΔG^0_{310}) were calculated with the program MeltWin 3.0.[45] The enzymatic hydrolysis of the oligonucleotides was performed as described[46] with snake venom phosphodiesterase (EC 3.1.15.1, *Crotallus adamanteus*) and alkaline phosphatase (EC 3.1.3.1, *Escherichia coli* from *Roche Diagnostics GmbH*, Germany) in 0.1 M Tris–HCl buffer (pH 8.3). Separation was carried out on reverse phase HPLC by gradient: 0.1 M (Et_3NH)OAc (pH 7.0)–MeCN 90:10, flow rate 1.0 mL/min.

4.1.3.1. 7-(2-Deoxy-β-D-*erythro*-pentofuranosyl)-7*H*-imidazo[1,2-*c*]-pyrrolo[2,3-*d*]-pyrimidine (12b). To 7-deaza-2′-deoxyadenosine (**5a**) (2 g, 8 mmol) was added chloroacetaldehyde (30 mL), and the solution was stirred for 18 h at 30 °C. After evaporation, flash chromatography (FC) on silica gel (column: 15×3 cm, CH_2Cl_2–CH_3OH 9:1) and crystallization from MeOH–EtOAc, colorless crystals (1.3 g, 65%) were obtained; mp 168–169 °C; TLC: R_f (CH_2Cl_2–CH_3OH 4:1) 0.8. UV (MeOH): λ_{max} 290 (5800), 240 (29,600). ^{1}H NMR (DMSO-d_6): 2.28 (m, 1H, H_α-C(2′)); 2.55 (m, 1H, H_β-C(2′)); 3.54 (m, 2H, H_2-C(5′)); 3.84 (s, 1H, H-C(4′)); 4.37 (s, 1H, H-C(3′)); 4.95 (t, *J*=5.5 Hz, 1H, HO-C(5′)); 5.33 (d, *J*=4.1 Hz, 1H, HO-C(3′)); 6.64 (t, *J*=6.1 Hz, 1H, H-C(1′)); 6.79 (d, *J*=3.5 Hz, 1H, H-C(9)); 7.46 (s, 1H, H-C(3)); 7.63 (d, *J*=3.2 Hz, 1H, H-C(8)); 7.95 (s, 1H, H-C(2)); 9.13 (s, 1H, H-C(5)). Anal. Calcd for $C_{13}H_{14}N_4O_3$ (274.28): C, 56.93; H, 5.14; N, 20.43. Found: C, 57.15; H, 5.02; N, 19.92.

4.1.3.2. 7-[2-Deoxy-5-*O*-(4,4′-dimethoxytriphenylmethyl)-β-D-*erythro*-pentofuranosyl]-7*H*-imidazo[1,2-*c*]-pyrrolo[2,3-*d*]pyrimidine (13). Compound **12b** (270 mg, 1 mmol) was dried by repeated co-evaporation with pyridine and then dissolved in dry pyridine (1 mL). To this solution 4,4′-dimethoxytriphenylmethyl-chloride (410 mg, 1.2 mmol) was added, and the solution was stirred at rt. After 4 h, the reaction was quenched by the addition of MeOH (1 mL). After further 10 min stirring, aq $NaHCO_3$ solution (5%, 5 mL) was added. The product was extracted with CH_2Cl_2 (3×20 mL). The combined organic phase was dried (Na_2SO_4), filtered, and the solvent was evaporated. After chromatography on silica gel (column: 10×3 cm, CH_2Cl_2–acetone 7:3) and evaporation of the main zone, the title compound **13** was obtained as a colorless foam (420 mg, 73%); TLC: R_f (CH_2Cl_2–acetone, 85:15) 0.33. ^{1}H NMR (DMSO-d_6): 2.35 (m, 1H, H_α-C(2′)); 2.64 (m, 1H, H_β-C(2′)); 3.18 (m, 2H, H_2-C(5′)); 3.70 (s, 6H, $2OCH_3$); 3.99 (m, 1H, H-C(4′)); 4.42 (m, 1H, H-C(3′)); 5.41 (d, *J*=4.4 Hz, 1H, HO-C(3′)); 6.69 (pt, *J*=6.5 Hz, 1H, H-C(1′)); 6.77–7.56 (m, 16H, 13 phenyl-H, H-C(9), H-C(3), H-C(8)); 7.98 (s, 1H, H-C(2)); 9.11 (s, 1H, H-C(5)). Anal. Calcd for $C_{34}H_{32}N_4O_5$ (576.65): C, 70.81; H, 5.59; N, 9.72. Found: C, 70.61; H, 5.43; N, 9.64.

4.1.3.3. 7-[2-Deoxy-5-*O*-(4,4′-dimethoxytriphenylmethyl)-β-D-*erythro*-pentofuranosyl]-7*H*-imidazo[1,2-*c*]-pyrrolo[2,3-*d*]pyrimidine 3′-(2-cyanoethyl *N*,*N*-diisopropylphosphoramidite) (14). Compound **13** (242 mg, 0.42 mmol) was dissolved in dry CH_2Cl_2 (1 mL). To the solution were added *N*,*N*-diisopropylethylamine (140 μL, 0.84 mmol) and chloro-(2-cyanoethoxy)-*N*,*N*-diisopropylaminophosphane (125 μL, 0.55 mmol). After stirring for 30 min at rt, aq $NaHCO_3$ solution (5%, 5 mL) was added. The product was extracted with CH_2Cl_2 (2×20 mL); the combined organic phase was dried (Na_2SO_4), filtered, and the solvent evaporated. After FC on silica gel (column: 10×3 cm, CH_2Cl_2–acetone 7:3) and evaporation, compound **14** was obtained as a colorless foam (208 mg, 64%); TLC: R_f (CH_2Cl_2–acetone 4:1) 0.63. ^{31}P NMR ($CDCl_3$): 150.00, 149.81.

4.1.3.4. Pyrrolo[2,3-*d*]pyrimidin-3*H*-2-one (19). 2-Methoxy-7*H*-pyrrolo[2,3-*d*]pyrimidine (**18**)[5] (900 mg, 6.04 mmol) was dissolved in concd HCl (20 mL) and the mixture was kept stirring under reflux for 1 h. After cooling, the solution was diluted with water (10 mL), filtered, and the filtrate was neutralized with aqueous ammonia yielding colorless needles, which were filtered off and dried (790 mg, 97%); mp 255 °C (dec.); TLC: R_f (CH_2Cl_2–CH_3OH 5:1) 0.47. UV (MeOH): $\lambda_{max}(\varepsilon)$=337 (2400), 295 (1200), 225 (18,600). ^{1}H NMR (DMSO-d_6): 6.20 (d, *J*=2.35 Hz, 1 H, H-C(5)); 7.07 (d, *J*=2.35 Hz, 1 H, H-C(6)); 8.18 (s, 1H, H-C(4)); 11.33 (br s, 2H, H-N(7), H-N(3)). Anal. Calcd for $C_6H_4N_3O$ (135.12): C, 53.33; H, 3.73; N, 31.10. Found: C, 53.21; H, 3.80; N, 30.90.

4.1.3.5. 3-(2,3,5-Tri-*O*-benzoyl-β-D-ribofuranosyl)-3,7-dihydro-pyrrolo[2,3-*d*]pyrimidin-3*H*-2-one (21). *N*,*O*-Bis(trimethylsilyl)acetamide (BSA, 0.21 mL, 0.82 mmol) was added to a stirred suspension of the pyrrolo[2,3-*d*]pyrimidin-2(3*H*)-one (**19**) (100 mg, 0.74 mmol) in dry MeCN (5 mL). After stirring at rt for 10 min, 1-*O*-acetyl-2,3,5-tri-*O*-benzoyl-β-D-ribofuranose (**20**, 0.41 g, 0.81 mmol) was added, followed by the addition of trimethylsilyl trifluoromethanesulfonate (0.15 mL, 0.82 mmol). The reaction was stirred at rt for 15 min and the flask was transferred to a preheated oil bath at 80 °C. After stirring for 1 h at 80 °C, the reaction was monitored by TLC. The reaction mixture was cooled to rt and diluted with EtOAc (40 mL), washed with satd $NaHCO_3$ and brine. Then the organic phase was dried over $MgSO_4$, filtered, and the solvent was removed under vacuum. The residue was purified by FC (silica gel, column 8×2.5 cm, CH_2Cl_2–CH_3OH 30:1). Evaporation of the main zone yielded a colorless foam, which was crystallized from EtOAc affording colorless crystals (372 mg, 87%); mp 219 °C (dec.); TLC: R_f (CH_2Cl_2–CH_3OH, 10:1) 0.50. UV (MeOH): $\lambda_{max}(\varepsilon)$=347 (2600), 274 (7400), 230 (56,600). ^{1}H NMR (DMSO-d_6): 4.66–4.84 (m, 3H, H_2-C(5′), H-C(4′)); 5.98 (m, 2H, H-C(2′)), H-C(3′)); 6.12 (d, *J*=3.6 Hz, 1H, H-C(5)); 6.33 (s, 1H, H-C(1′)); 7.15 (d, *J*=3.76 Hz, 1H, H-C(6)); 7.39–8.03 (m, 15 H-ph); 8.58 (s, 1H, H-C(4)); 11.31 (br s, 1H, H-N(7)). Anal. Calcd for $C_{32}H_{25}N_3O_8$ (579.56): C, 66.32; H, 4.35; N, 7.52. Found: C, 66.30; H, 4.31; N, 7.30.

4.1.3.6. 3-(β-D-Ribofuranosyl)-3,7-dihydro-pyrrolo[2,3-*d*]pyrimidin-3*H*-2-one (7a). 3-(2,3,5-Tri-*O*-benzoyl-β-D-ribofuranosyl)pyrrolo[2,3-*d*]pyrimidin-3*H*-2-one (**21**, 320 mg, 0.55 mmol) was suspended in 0.5 M NaOMe in methanol (100 mL). The mixture was stirred at rt overnight. TLC showed the completion of the reaction. The mixture was evaporated, the residue was dissolved in H_2O and the solution was neutralized with 1 N AcOH. It was evaporated to dryness and was applied on to FC (silica gel, column

8×2.5 cm, CH_2Cl_2–CH_3OH 4:1), furnishing a colorless solid. Crystallization from MeOH–CH_2Cl_2 afforded slightly pink crystals (120 mg, 81%); mp 188 °C (dec.); TLC: R_f (CH_2Cl_2–CH_3OH 4:1) 0.45. UV (MeOH): $\lambda_{max}(\varepsilon)$ 344 (3100), 274 (3800), 227 (21,500). ^{1}H NMR (DMSO-d_6): 3.61–3.82 (m, 2H, H_2-C(5′)); 3.94–3.99 (m 3H, H-C(4′), H-C(2′), H-C(3′)); 5.00 (s, 1H, OH-C(5′)); 5.23 (s, 1H, OH-C(3′)); 5.48 (s, 1H, OH-C(2′)); 5.92 (s, 1H, H-C(1′)); 6.20 (d, J=3.4 Hz, 1H, H-C(5)); 7.10 (d, J=3.4 Hz, 1H, H-C(6)); 8.81 (s, 1H, H-C(4)); 11.16 (br s, 1H, H-N(7)). Anal. Calcd for $C_{11}H_{13}N_3O_5$ (267.24): C, 49.44; H, 4.90; N, 15.72. Found: C, 49.22; H, 5.10; N, 15.55.

4.1.3.7. 5-(Hept-1,6-diynyl)-2′-deoxyuridine (16). To a suspension of 5-iodo-2′-deoxyuridine (**15**, 0.5 g, 1.41 mmol) and CuI (54 mg, 0.28 mmol) in anhydrous DMF (8 mL) were added successively 1,6-heptadiyne (1.3 g, 14.1 mmol), anhydrous Et_3N (283 mg, 2.8 mmol), and Pd(0)(PPh_3)$_4$ (162 mg, 0.14 mmol). The mixture was stirred at rt for 16 h under argon atmosphere. The reaction mixture was diluted with MeOH–CH_2Cl_2 (1:1, 30 mL), and Dowex 1X8 (100–200 mesh; 0.5 g, bicarbonate form) was introduced. After additional stirring for 1 h, the mixture was filtered and the resin washed with MeOH–CH_2Cl_2 1:1, 50 mL. The combined filtrates were evaporated, and the residue was purified by FC (silica gel, column 15×3 cm, CH_2Cl_2–MeOH 96:4) affording **16** as a colorless amorphous solid (0.34 g, 76%). TLC: R_f (CH_2Cl_2–MeOH 9:1) 0.50. UV (MeOH): $\lambda_{max}(\varepsilon)$ 229 (14,500), 292 (14,800). ^{1}H NMR (DMSO-d_6): 1.69–1.73 (m, 2H, CH_2); 2.14–2.47 (m, 6H, 2CH_2, H_2-C(2′)); 2.87 (s, 1H, C≡CH); 3.63 (m, 2H, H_2-C(5′)); 3.83 (m, 1H, H-C(4′)); 4.27 (m, 1H, H-C(3′)); 5.15 (m, 1H, OH-C(5′)); 5.29 (m, 1H, OH-C(3′)); 6.15 (m, 1H, H-C(1′)); 8.19 (s, 1H, H-C(6)); 11.62 (s, 1H, H-N(7)). Anal. Calcd for $C_{16}H_{18}N_2O_5$ (318.12): C, 60.37; H, 5.70; N, 8.80. Found: C, 60.26; H, 5.75; N, 8.85.

4.1.3.8. 3-(2-Deoxy-β-D-*erythro*-pentofuranosyl)-6-pentyn-1-yl-furo[2,3-*d*]pyrimidin-3*H*-2-one (17). To a solution of compound **16** (200 mg, 0.63 mmol) in Et_3N–MeOH (3:7, 30 mL) was added CuI (21 mg, 0.11 mmol) and the mixture was refluxed for 6 h. The solvent was evaporated in vacuo and the crude product was purified by FC (silica gel, column 15×3 cm, CH_2Cl_2–MeOH, 95:5) to give a colorless amorphous solid (180 mg, 90%); TLC: R_f (CH_2Cl_2–MeOH 9:1) 0.45. UV (MeOH): $\lambda_{max}(\varepsilon)$ 244 (10,000), 331 (5600). ^{1}H NMR (DMSO-d_6): 1.79 (m, 2H, CH_2); 2.04 (m, 1H, H_α-C(2′)); 2.23 (m, 2H, CH_2); 2.26 (m, 1H, H_β-C(2′)); 2.73 (t, J=7.4 Hz, 2H, CH_2); 2.84 (s, 1H, C≡CH); 3.35 (m, 2H, H_2-C(5′)); 3.89 (m, 1H, H-C(4′)); 4.22 (m, 3H, H-C(3′)); 5.13 (m, 1H, OH-C(5′)); 5.28 (1H, OH-C(3′)); 6.16 (t, J=6.10 Hz, 1H, H-C(1′)); 6.47 (s, 1H, H-C(5)); 8.68 (s, 1H, H-C(4)).

4.1.3.9. 3-(2-Deoxy-β-D-*erythro*-pentofuranosyl)-3,7-dihydro-6-pentyn-1-yl-pyrrolo[2,3-*d*]pyrimidin-2-one (7d). Compound **17** (200 mg, 0.62 mmol) was dissolved in concd aqueous NH_3 (30 mL) and the reaction mixture was stirred at rt overnight. The resulting solution was concentrated and the residue applied to FC (silica gel, column 15×3 cm, CH_2Cl_2–MeOH 9:1) to give **7d** as a colorless foam (184 mg, 92%). TLC: R_f (CH_2Cl_2–MeOH 9:1) 0.21. UV (MeOH): λ_{max} 229 (24,600), 262 (4000), 343 (4000). ^{1}H NMR (DMSO-d_6): 1.76–1.81 (m, 2H, CH_2); 1.98 (m, 1H, H_α-C(2′)); 2.19–2.33 (m, 3H, CH_2, H_β-C(2′)); 2.59–2.64 (t, J=6.7 Hz, 2H, CH_2); 2.83 (s, 1H, C≡CH), 3.63 (m, 2H, H_2-C(5′)); 3.86 (m, 1H, H-C(4′)); 4.23 (m, 1H, H-C(3′)); 5.10 (m, 1H, OH-C(5′)); 5.25 (m, 1H, OH-C(3′)); 5.93 (s, 1H, H-C(7)); 6.25 (t, J=6.10 Hz, 1H, H-C(1′)); 8.51 (s, 1H, H-C(6)); 11.1 (s, 1H, H-N(7)). Anal. Calcd for $C_{16}H_{19}N_3O_4$ (317.34): C, 60.56; H, 6.03; N, 13.24. Found: C, 60.46; H, 6.04; N, 13.08.

Acknowledgements

We thank Mrs. Simone Budow for measuring some of the NMR spectra and Mr. Gabiele De Paoli for his help in fluorescence measurement. Financial support by ChemBiotech is gratefully acknowledged.

References and notes

1. Callis, P. R. *Annu. Rev. Phys. Chem.* **1983**, *34*, 329–357.
2. Ward, D. C.; Reich, E. *J. Biol. Chem.* **1969**, *244*, 1228–1237.
3. Seela, F.; Steker, H.; Driller, H.; Bindig, U. *Liebigs Ann. Chem.* **1987**, 15–19.
4. Seela, F.; Steker, H. *Liebigs Ann. Chem.* **1984**, 1719–1730.
5. Seela, F.; Chen, Y.; Bindig, U.; Kazimierczuk, Z. *Helv. Chim. Acta* **1994**, *77*, 194–202.
6. (a) Lindahl, T. *Nature* **1993**, *362*, 709–715; (b) Wierzchowski, J.; Wielgus-Kutrowska, B.; Shugar, D. *Biochim. Biophys. Acta* **1996**, *1290*, 9–17.
7. Winkeler, H.-D.; Seela, F. *Liebigs Ann. Chem.* **1984**, 708–721.
8. Seela, F.; Chen, Y. *Helv. Chim. Acta* **1997**, *80*, 1073–1086.
9. Seela, F.; Zulauf, M.; Sauer, M.; Deimel, M. *Helv. Chim. Acta* **2000**, *83*, 910–927.
10. Okamoto, A.; Tanaka, K.; Fukuta, T.; Saito, I. *J. Am. Chem. Soc.* **2003**, *125*, 9296–9297.
11. Okamoto, A.; Tanaka, K.; Saito, I. *J. Am. Chem. Soc.* **2004**, *126*, 9458–9463.
12. Woo, J.; Meyer, R. B., Jr.; Gamper, H. B. *Nucleic Acids Res.* **1996**, *24*, 2470–2475.
13. Secrist, J. A., III; Barrio, J. R.; Leonard, N. J.; Weber, G. *Biochemistry* **1972**, *11*, 3499–3506.
14. Srivastava, S. C.; Raza, S. K.; Misra, R. *Nucleic Acids Res.* **1994**, *22*, 1296–1304.
15. Zhang, W.; Rieger, R.; Iden, C.; Johnson, F. *Chem. Res. Toxicol.* **1995**, *8*, 148–156.
16. (a) Kasai, H.; Goto, M.; Ikeda, K.; Zama, M.; Mizuno, Y.; Takemura, S.; Matsuura, S.; Sugimoto, T.; Goto, T. *Biochemistry* **1976**, *15*, 898–904; (b) Sattsangi, P. D.; Leonard, N. J.; Frihart, C. R. *J. Org. Chem.* **1977**, *42*, 3292–3296.
17. Bazin, H.; Zhou, X.-X.; Glemarec, C.; Chattopadhyaya, J. *Tetrahedron Lett.* **1987**, *28*, 3275–3278.
18. Seela, F.; Bussmann, W. *Tetrahedron* **1985**, *41*, 935–940.
19. Inoue, Y.; Kuramochi, T.; Imakubo, K. *Chem. Lett.* **1981**, 1161–1164.
20. (a) Sugiyama, T.; Schweinberger, E.; Kazimierczuk, Z.; Ramzaeva, N.; Rosemeyer, H.; Seela, F. *Chem.—Eur. J.* **2000**, *6*, 369–378; (b) Yip, K.-F.; Tsou, K.-C. *J. Org. Chem.* **1975**, *40*, 1066–1070.
21. (a) Seela, F.; Lindner, M.; Glaçon, V.; Lin, W. *J. Org. Chem.* **2004**, *69*, 4695–4700; (b) Lin, W.; Li, H.; Ming, X.; Seela, F. *Org. Biomol. Chem.* **2005**, *3*, 1714–1718; (c) Bhat, G. A.;

Townsend, L. B. *J. Chem. Soc., Perkin Trans. 1* **1981**, 2387–2393.
22. (a) Bhat, G. A.; Schram, K. H.; Townsend, L. B. *J. Carbohydr. Nucleosides Nucleotides* **1980**, *7*, 333–345; (b) Seela, F.; Rosemeyer, H.; Schweinberger, E. Deutsche Offenlegungsschrift DE 102004009977A1, September 22, 2005.
23. Rist, M. J.; Marino, J. P. *Curr. Org. Chem.* **2002**, *6*, 775–793.
24. (a) Leonard, N. J.; Tolman, G. L. *Ann. N.Y. Acad. Sci.* **1975**, *255*, 43–58; (b) Lorente, C.; Thomas, A. *Acc. Chem. Res.* **2006**, *39*, 395–402.
25. Kochetkov, N. K.; Shibaev, V. N.; Kost, A. A. *Tetrahedron Lett.* **1971**, *12*, 1993–1996.
26. Barrio, J. R.; Secrist, J. A., III; Leonard, N. J. *Biochem. Biophys. Res. Commun.* **1972**, *46*, 597–604.
27. Seela, F.; Kehne, A. *Liebigs Ann. Chem.* **1983**, 876–884.
28. Schaller, H.; Weimann, G.; Lerch, B.; Khorana, H. G. *J. Am. Chem. Soc.* **1963**, *85*, 3821–3827.
29. Beaucage, S. L.; Caruthers, M. H. *Tetrahedron Lett.* **1981**, *22*, 1859–1862.
30. Hudson, R. H. E.; Dambenieks, A. K.; Viirre, R. D. *Synlett* **2004**, 2400–2402.
31. Loakes, D.; Brown, D. M.; Salisbury, S. A.; McDougall, M. G.; Neagu, C.; Nampalli, S.; Kumar, S. *Helv. Chim. Acta* **2003**, *86*, 1193–1204.
32. Seela, F.; Sirivolu, V. R. *Chem. Biodivers.* **2006**, *3*, 509–514.
33. Srinivasan, S.; McGuigan, C.; Andrei, G.; Snoeck, R.; De Clercq, E.; Balzarini, J. *Bioorg. Med. Chem. Lett.* **2001**, *11*, 391–393.
34. Schram, K. H.; Townsend, L. B. *Tetrahedron Lett.* **1974**, *15*, 1345–1348.
35. Fletcher, A. N. *Photochem. Photobiol.* **1969**, *9*, 439–444.
36. Seela, F.; Münster, I.; Löchner, U.; Rosemeyer, H. *Helv. Chim. Acta* **1998**, *81*, 1139–1155.
37. Leonard, G. A.; McAuley-Hecht, K. E.; Gibson, N. J.; Brown, T.; Watson, W. P.; Hunter, W. N. *Biochemistry* **1994**, *33*, 4755–4761.
38. Guckian, K. M.; Schweitzer, B. A.; Ren, R. X.-F.; Sheils, C. J.; Tahmassebi, D. C.; Kool, E. T. *J. Am. Chem. Soc.* **2000**, *122*, 2213–2222.
39. Rosemeyer, H.; Seela, F. *J. Chem. Soc., Perkin Trans. 2* **2002**, 746–750.
40. Kool, E. T. *Chem. Rev.* **1997**, *97*, 1473–1487.
41. Rosemeyer, H.; Mokrosch, V.; Jawalekar, A.; Becker, E.-M.; Seela, F. *Helv. Chim. Acta* **2004**, *87*, 536–553.
42. Seela, F.; He, Y. In *Modified Nucleosides, Synthesis and Applications*; Loakes, D., Ed.; Research Signpost: Kerala, India, 2002; pp 57–85.
43. Nordlund, T. M.; Xu, D.; Evans, K. O. *Biochemistry* **1993**, *32*, 12090–12095.
44. Kouchakdjian, M.; Eisenberg, M.; Yarema, K.; Basu, A.; Essigmann, J.; Patel, D. J. *Biochemistry* **1991**, *30*, 1820–1828.
45. McDowell, J. A.; Turner, D. H. *Biochemistry* **1996**, *35*, 14077–14089.
46. Seela, F.; Lampe, S. *Helv. Chim. Acta* **1991**, *74*, 1790–1800.